

# Leukocyte Activation Assay Using AI-Enhanced Digital Holographic Microscopy

Kerem Delikoyun<sup>1,5\*</sup>, Qianyu Chen<sup>1,5</sup>, Johannes Krell<sup>2</sup>, Si Ko Myo<sup>1</sup>,  
Martin Schlegel<sup>2</sup>, Gerhard Schneider<sup>2</sup>, Matthew Cove<sup>3</sup>,  
John Soong Tshon Yit<sup>4</sup>, Klaus Diepold<sup>5</sup>, Oliver Hayden<sup>1,5</sup>

<sup>1</sup>TUMCREATE, Singapore

<sup>2</sup>Department of Anaesthesia, School of Medicine and Health, Technical University of Munich, München, Germany

<sup>3</sup>Division of Respiratory & Critical Care Medicine, Department of Medicine, National University Hospital, Singapore

<sup>4</sup>Division of Acute Internal Medicine, Department of Medicine, National University Hospital, Singapore

<sup>5</sup>School of Computation, Information and Technology, Technical University of Munich, München, Germany

\*kerem.delikoyun@tum-create.edu.sg

**Abstract** - Digital holographic microscopy (DHM) is a label-free and high-throughput cellular imaging technology leverages phase contrast to reveal subtle intercellular refractive index variations, allowing to the derivation of biophysical parameters related to cell function. Neutrophil and monocyte activation, major parts of the innate immune system, can be quantified via fluorescence flow cytometry by measuring activation markers, aiding in the diagnosis and assessment of inflammatory diseases. However, workflow standardization and quantification with fluorescence flow cytometry remain laborious, challenging, and costly. Automated haematology analysers are widely available, solve labour challenges, and provide economical differential leukocyte counts but cannot differentiate or assess leukocyte activation. There is an unmet need to provide reliable information on immune cell function at the bedside using point-of-care diagnostics. DHM potentially meets this need by providing label-free, automated, high-throughput and high-resolution cellular imaging capable of monitoring leukocyte activation. Furthermore, integrating deep learning models can be used to accurately recognize activated cells, reducing operator variability and automating analysis. We present a novel imaging platform utilizing DHM to identify activated leukocytes as an early predictive biomarker for inflammatory states, demonstrating this technology may enable real-time patient monitoring in clinical settings, facilitating risk stratification and therapy response monitoring at the bedside.

**Keywords:** Leukocyte activation, digital holographic microscopy, imaging flow cytometer, self-supervised learning, object detection

## 1. Introduction

The human immune system, a complex network of cells and proteins, is pivotal in protecting the body against infections and diseases. Among its components, leukocytes (white blood cells) are crucial for detecting and responding to pathogens. The innate immune system, especially monocytes and neutrophils (comprise up to 70% of all leukocytes), are essential in mounting effectively early immune responses against pathogens [1]. Activated monocytes differentiate into macrophages, which can acquire pro- or anti-inflammatory phenotypes based on stimuli they encounter. Especially classical proinflammatory monocytes infiltrate sites of inflammation after the detection of pathogens through specialised receptors and shape the inflammatory microenvironment through the release of proinflammatory cytokines [2]. Neutrophils, conversely, are infection first responders mediating immediate pathogen elimination and modulation of other immune cells [3].

Cellular immune activation is routinely traced in transplantation immunology and the monitoring of autoimmune diseases, with a focus primarily on the adaptive immune system. These tests have demonstrated potential in diagnosing and monitoring diseases characterized by immune dysregulation [4]. For instance, monocyte/macrophage activation tests have shown utility in conditions like subclinical atherosclerosis and breast cancer and assessment of neutrophil activation and subsequent immune response provide information about pathogen clearance and immune homeostasis. Neutrophils employ various mechanisms, including degranulation, phagocytosis, reactive oxygen species (ROS) production, and the release of

neutrophil extracellular traps (NETs) and extracellular vesicles (EVs). While essential for combating infections, these mechanisms can also lead to tissue damage if not properly regulated [5, 6]. They are also key players in immune regulation through the release of chemokines, cytokines and complement factors which are critical for the maturation and differentiation of the adaptive immune system through cellular cross talk. Neutrophil activation is usually triggered by the activation of Pattern Recognition Receptors (PPRs) on the cell surface, which detect tissue damage and various pathogens. This leads to neutrophil recruitment to the site of inflammation through the capillary wall. This is cellular shape change mediated by selectins and chemotaxis in multiple chemokine gradients. An important aspect of neutrophil activation features degranulation, which involves the recruitment of granules containing oxidative and non-oxidative antimicrobial agents to the cell surface membrane.

Given the complexity and significance of leukocyte activation in immune response and disease progression, advanced imaging techniques are essential for a detailed understanding of these processes. Traditional imaging methods, such as blood smear analysis and flow cytometry, have limitations regarding resolution, sample preparation, and time consumption. Automated haematology analysers resolve some issues, like time consumption, and are crucial for blood cell counting and characterization in clinical practice but are unable to provide detailed leukocyte activation analysis [7]. They primarily focus on basic morphology, missing specific activation markers and subtle changes in cell function. Flow cytometry is more detailed, but it requires labour-intensive sample preparation and complex labelling, and is therefore costly.

Digital holographic microscopy (DHM) has emerged as a novel cellular imaging tool, offering real-time, high throughput, and quantitative imaging capabilities without need for labelling. DHM captures the interference patterns of light waves passing through samples, revealing detailed cellular structures without staining, thus preserving cells in their native state and ensuring more accurate analysis [8]. Integrating deep learning algorithms for pattern recognition with DHM enhances its analytical power, allowing rapid image processing and interpretation of complex data and to rapidly identify biomarkers indicative of leukocyte activation.

This study describes the use of DHM enhanced with deep learning for analysing leukocyte activation, aiming to overcome limitations of traditional imaging technologies, and introducing a potential predictive biomarker for clinical practice. We showed that complex immune activation patterns can be effectively resolved and recognized using DHM, enabling time evolution studies to capture real-time activation dynamics. It is also presented that DHM brings a novel activation assay that enables the detection of activated cells and quantification of activation states within the population. We further validate our approach of analysing clinical samples from pneumonia and healthy patients, highlighting a clear correlation between the activated leukocytes and the severity of the disease. We envision that this novel tool could potentially improve diagnostics and personalized medicine through monitoring treatment efficacy, drug screening, and advancing research on immune cell behaviour and activation mechanisms.

## **2. Methods**

### **2.1. Digital Holographic Microscopy**

This study utilized a differential holographic microscope setup for cellular imaging (Ovizio Imaging Systems, Belgium). The microscope comprises a 528 nm Osilon PowerStar SLED (Osram) for partially coherent Koehler illumination and is fitted with a 40× objective with a numerical aperture (NA) of 0.55. A low-coherence light source significantly minimizes the noise, improving the image quality. When the light passes through the sample in the microfluidic channel under the flow, the scattered light is split by a diffraction grating into the reference (diffracted) and object (non-diffracted) waves. Afterwards, a wedge tweaks the reference wave to introduce an optical phase shift (Figure 1) [9]. Different from a typical Michelson interferometry, the setup uses a more robust and tight optical design, which is immune to environmental changes or operator influences and allows potential point-of-care applications in clinical settings.

We performed measurements in DHM using deidentified human whole blood samples from patients who provided written consent prior to blood draw in the Intensive Care Unit (ICU) and Emergency Department (ED) of the National University Hospital (NUH) in Singapore. The protocol was approved by the local Domain Specific Institutional Review

Board (DSIRB 2021-00930). The inclusion criteria for the study were: age above 18, body temperature above 38.5 °C, no autoimmune disease, no malignant disease, and no HIV infection.

We collected 2 ml of citrated peripheral whole blood from each patient who met these criteria and gave informed consent. The collected whole blood samples were diluted with the ratio of 1:100 in phosphate-buffered saline (PBS, Sigma Aldrich, USA) containing 0.05% polyethylene oxide ( $4 \times 10^6$  Da, Sigma Aldrich, USA) to ensure that all blood cells are viscoelastically focused to a uniform plane without losing any optical cellular information and need for continuous focusing. For each sample, we collected 3 sets of 10,000 frames at an acquisition rate of 105 frames per second to obtain sufficient event.

## 2.2. Microfluidics

The microfluidic chip contains a straight channel with cross-sectional dimensions of  $50 \mu\text{m} \times 500 \mu\text{m}$  for imaging under DHM. The sheath buffers from top/bottom and left/right are introduced to tightly focus the sample flowing at a uniform plane within the field of view of the microscope objective. The flow rates of the sample and top/bottom sheath buffers are set to  $0.2 \mu\text{l/s}$  with a left/right sheath buffer of  $0.5 \mu\text{l/s}$ . This flow regime provides an even focusing plane at the order of the microscope objective's depth of field (DOF) of  $\pm 2.3 \mu\text{m}$  [8], ensuring that relatively minor fluctuations do not affect the optical focus and cause any significant cellular information.

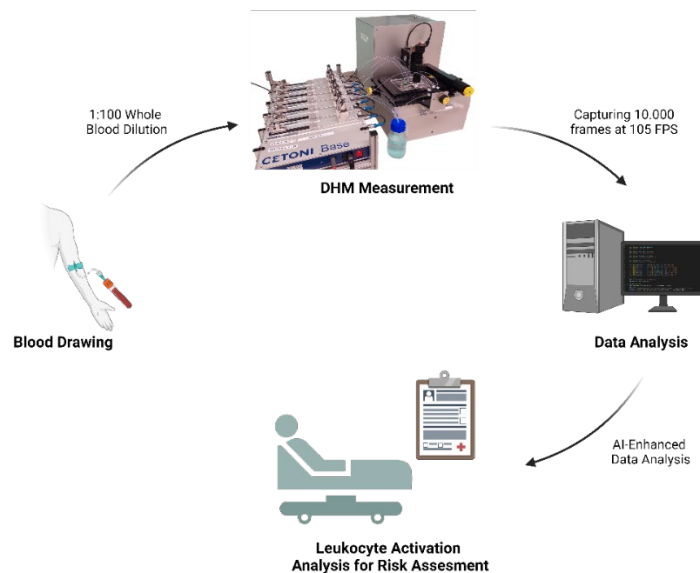


Fig. 1: The overall schematic and workflow of DHM.

## 2.3. DHM Experiments and Data Analysis

### Dataset Preparation

In this study, two different experimental protocols were followed to develop different deep learning models: *i)* stimulation of neutrophils to quantify activation stages for time evolution study and *ii)* stimulation of neutrophils and monocytes to develop another model to detect activated leukocytes in clinical samples from healthy control and fever patients. For each group, neutrophils and monocytes were isolated using a magnetic cell sorting kit (Miltenyi, USA) to isolate “untouched” cells through negative depletion from whole blood of health donors. Additionally, an erythrocyte depletion kit was employed to increase the purity of the sorted cells following negative depletion. After isolating the target cells, neutrophils were split and treated with  $10 \mu\text{g/ml}$  of Lipopolysaccharides from *Pseudomonas aeruginosa* (Sigma Aldrich,

USA) or with PMA (phorbol 12-myristate-13-acetate) and ionomycin (100 nM) for stimulation. Cells were incubated in RPMI 1640 at 37 °C in a physiological calcium concentration and time evolution measurements were conducted with DHM up to 120 min with 15 min intervals to observe the kinetics of morphological changes. Validation measurements were performed using a fluorescence imaging flow cytometer (Cytek Amnis ImageStream X Mark II, USA), with staining against CD45, CD 69, HLA-DR and CD66B.

The data acquisition and hologram reconstruction in DHM were performed using API provided by the manufacturer. The phase images containing unstimulated and stimulated cells were carefully annotated to ensure that each bounding box accurately encompassed the cell with the corresponding class in YOLO format. The annotation process involved manual examination of each frame to identify and label the cells with respective classes. Firstly, a small training set was generated to train the YOLOv8x object detection model. Afterwards, this model was used to automate the annotation process [10]. The annotator's hen performed a quality check over annotations and minor corrections to expand the dataset. Therefore, the final dataset comprises 18,000 annotated frames for treated and untreated neutrophils and monocytes. Each frame captures the unique morphological characteristics of the cells, which is crucial for learning the intricate patterns associated with leukocyte activation. Furthermore, each neutrophil covered by bounding boxes was cropped (50-pixel x 50-pixel) to study the effect of time evolution and quantification of activation stages.

### **Self-supervised learning using autoencoder to quantify activation stages of neutrophils over time**

An autoencoder was trained to extract valuable features from unlabelled data over time. The autoencoder was employed to learn a compressed representation of the input phase images of neutrophils. This model was composed of an encoder, which reduced the dimensionality of the data by capturing the most significant features, and a decoder, which attempted to reconstruct the original input from these features by sampling. Training the autoencoder on phase images of unstimulated and stimulated neutrophils without giving any explicit label taught it to capture the essential morphological changes associated with different activation stages.

After training, the high-dimensional features extracted by the autoencoder were further reduced using Principal Component Analysis (PCA), ensuring that the most critical information was retained while eliminating noise. The reduced-dimensionality features were then clustered using the K-Means clustering algorithm, which categorized the data points into three distinct groups: unstimulated, intermediate, and stimulated neutrophils. This approach allowed the model to automatically detect and quantify the activation stages of neutrophils over time without the need for extensive manual annotation. The model's effectiveness was validated by comparing its classification results with ground truth labels (i.e., time points) to quantify the activation stages of neutrophils.

### **Developing an object detection framework for identifying activated leukocytes in clinical samples**

An object detection model was trained to analyse clinical samples from healthy and fever patients to quantify activated leukocytes. The YOLOv8x object detection framework was chosen for its balance between accuracy and speed, making it suitable for real-time analysis. The dataset included phase images of various blood cells, such as erythrocytes, platelets, and white blood cells, to ensure the model's robustness in recognizing different cell types. Special attention was given to neutrophils and monocytes in their resting and activated states by including stimulated samples in the training set.

During training, the network learned to identify and localize leukocytes within the phase images, distinguishing between healthy and activated cells. This process involved extensive data augmentation techniques to simulate the variability found in clinical samples and enhance the model's generalization capabilities. Various object detection architectures were evaluated, with the model demonstrating the highest precision and recall selected for the final application. The chosen model was then validated on independent clinical samples, proving its ability to accurately detect activated leukocytes.

### **Implementation of deep learning frameworks**

*i)* The Variational Autoencoder (VAE) model was implemented using Python (v3.10.6) and PyTorch (v2.2.2), trained on a system with an i7-12800H CPU, 32 GB RAM, and an NVIDIA RTX 3080 Ti GPU. The VAE featured an encoder with four convolutional layers and a decoder mirroring the encoder. Training involved a custom loss function combining binary cross-entropy and Kullback-Leibler divergence, optimized with the Adam optimizer and a cosine annealing scheduler.

Gradient clipping and L2 regularization were used to enhance training stability and prevent overfitting. A grid search was conducted to optimize hyperparameters, resulting in the best model configuration based on the lowest validation loss.

*ii)* Object detection models were trained using Ultralytics (v8.2.26) on the same system. Hyperparameter tuning through grid search focused on the learning rate, batch size, dropout rate, and optimizer configuration, with the batch size consistently set to 16. Training employed the Adam optimizer with an initial learning rate of 0.01 and a decaying learning rate strategy. A dropout rate of 0.1 was used to prevent overfitting.

Table 1: Validation Results of Different Object Detection Models

	Precision	Recall	mAP50	mAP95
RT-DETR	86.7%	94.4%	87.4%	71.3%
YOLOv9e	93.4%	94.3%	95.2%	91.1%
<b>YOLOv8x</b>	<b>94.8%</b>	<b>97.9%</b>	<b>95.2%</b>	<b>91.8%</b>

### 3. Results and Discussion

This manuscript evaluated the application of digital holographic microscopy (DHM) coupled with deep learning algorithms for the analysis of leukocyte activation. Our results demonstrate that DHM can effectively capture high-resolution, label-free images of leukocytes, providing detailed insights into their morphological changes upon activation. The integration of deep learning models facilitated the precise recognition of activated cells, significantly enhancing the analytical capabilities of DHM. The platform successfully detected morphological changes in neutrophils stimulated with lipopolysaccharide (LPS). Using an autoencoder, we extracted the most discriminative features unsupervised without explicitly training the model with labels. This autoencoder-based model was tested on time-evolution data, clustering cell populations into three groups: unstimulated, intermediate, and stimulated, without predefined boundary conditions. The model effectively categorized each sample into its respective group, as depicted in Figure 3A.

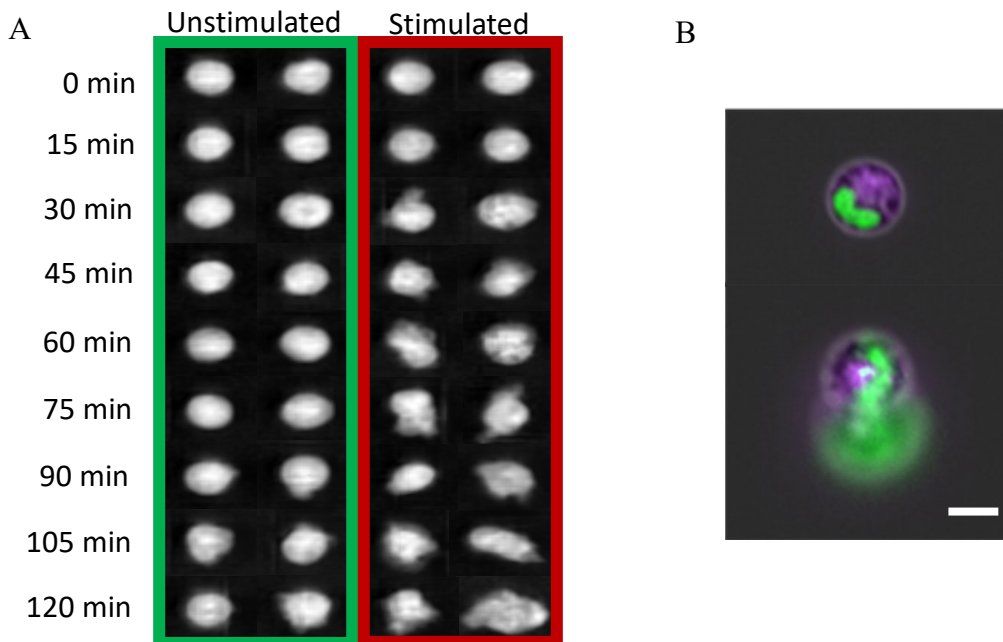


Fig. 2: Time evolution of neutrophil activation: a) morphological changes over time between unstimulated and stimulated (10  $\mu\text{g/ml}$  LPS) neutrophils captured using DHM and b) Unstimulated (above) and stimulated (below) neutrophils. The cell membrane rupture and leaky nucleus following stimulation were confirmed using fluorescence imaging flow cytometer. Green: DNA dye and purple: CD66b. Scale bar: 10  $\mu\text{m}$ .

Initially, the unstimulated group is well above 80%, with a small group of unavoidable and inherent activated neutrophils present in the sample due to donor, isolation protocol or sample handling. The intermediate stage exhibited overlap with the stimulated and unstimulated groups, which is expected due to the subtle transition features between these stages (Figure 3A). Therefore, we defined an intermediate stage for these ambiguous transitional features. The overlapping samples between groups can be attributed to minor morphological changes. The stages were proposed based on DHM data and the clustering results from the trained autoencoder. However, these stages align with the kinetics described in the literature, where upon NETosis activation, neutrophils undergo chromatin expansion within the nucleus, rupture of the nuclear membrane, and leakage into the cytoplasm, typically taking around 100 minutes. Subsequently, NETs rupture the cell membrane and spread (>100 minutes) [11].

This process is highlighted by the spike observed at the 105-minute time (Figure 3B), where leaky and spiky edges become more pronounced (Figure 2A). Although nuclear membrane changes are not directly visible in phase images, our model could recognize intracellular changes and classify most structures as the intermediate stage until significant changes occur on the cell membrane. Concurrently, the unstimulated cell population sharply decreased to below 20%, as expected. The intermediate stage population increased, reaching a plateau at around 60 minutes before decreasing as more neutrophils became activated after around 100 min, indicated by increasing population percentages. Note that our workflow allows us to screen cells under flow at high throughput, in contrast to studies performed by fluorescence or confocal imaging with attached cells. Therefore, cell morphologies observed in DHM do not necessarily follow the same morphological pattern described before; in fact, this scheme enables us to determine and cluster the activation stages of neutrophils in a real-time and label-free fashion.

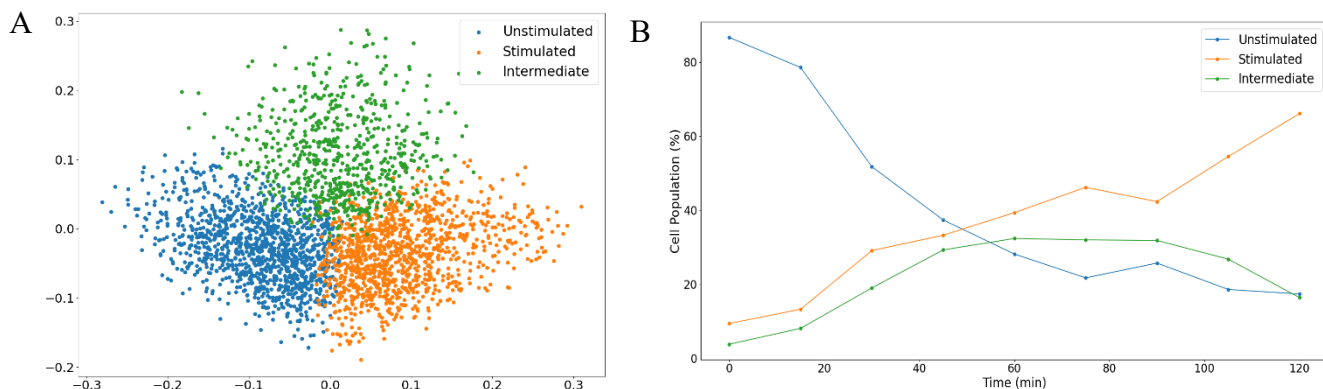


Fig. 3: Quantifying the unstimulated, intermediate, and stimulated neutrophils over time using self-supervised learning. a) Clustered cell populations after extracting self-supervised features and b) prediction of time points of each sample over incubation time.

We analysed blood samples from healthy controls and fever patients to validate our approach. We developed a deep learning framework trained using data from erythrocytes, platelets, and unstimulated and stimulated neutrophils and monocytes. Given that our model could effectively recognize leukocyte activation patterns, as demonstrated in Figure 2A, we did not need to train the model with every leukocyte subtype. Instead, the model learned the common features inherent to different leukocyte classes and their activation morphologies (Figure 4A). The effect of leukocyte type and size on the model's performance and clinical outcomes is reserved for future studies.

Subsequently, we analysed clinical samples after performing a comparative study between various object detection models trained on the same dataset (Table 1). These samples were obtained from healthy controls and fever patients, comprising four groups. The results revealed a significant increase and a broader distribution in the number of activated leukocytes detected in fever patients compared to healthy individuals ( $p < 0.1$ ). Specifically, the average percentage of activated leukocytes in healthy controls was approximately 5.41%, whereas it was 32.38% in fever patients (Figure 4B).

Notably, the distribution of activated cells among fever patients was quite variable, ranging from as high as 62% to as low as 11%. In contrast, the distribution in healthy controls was much narrower. This variability in fever patients underscores the heterogeneity of immune responses during fever and suggests that while some patients exhibit a pronounced leukocyte activation, others may have a more restrained response. These findings validate our model's effectiveness in detecting activated leukocytes and highlight its potential utility in clinical settings for monitoring immune responses. The ability to differentiate between healthy and fever states based on leukocyte activation patterns could be instrumental in early diagnosis and treatment monitoring of inflammatory conditions. However, we still need to validate and generalize our findings with a larger cohort of patients. Expanding the sample size will help ensure the robustness of our model and its applicability across diverse patient populations. This will also provide a deeper understanding of the variability in immune responses among different individuals, further refining our approach's diagnostic and prognostic capabilities.

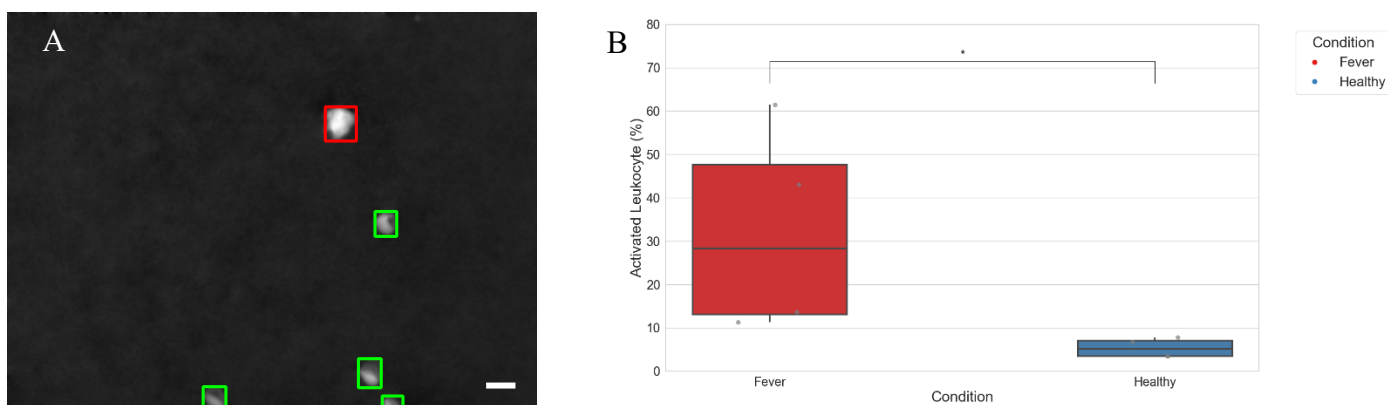


Fig. 4: Detecting activated leukocytes in clinical samples from healthy control and fever patient samples. a) detected cells by object detection model, activated leukocyte (red), erythrocytes (green), indicated with bounding boxes, b) the quantified comparison of activated leukocyte percentages between healthy control and fever patient samples,  $p$ -value $<0.1$ . Scale bar: 10  $\mu$ m.

## 5. Conclusion

The present study demonstrates the efficacy of digital holographic microscopy (DHM) integrated with deep learning algorithms in analysing leukocyte activation. DHM's ability to capture high-resolution, label-free images of leukocytes, coupled with the deep learning model's precision in recognizing activated cells, offers a significant advancement in the analytical capabilities of cellular imaging technologies. Using an autoencoder, we extracted the most discriminative features of neutrophil activation in an unsupervised manner. This approach allowed the model to categorize leukocyte activation stages: unstimulated, intermediate, and stimulated based on morphological changes without predefined labels. Clustering cell populations into these distinct groups align with known biological processes such as NETosis, where neutrophils undergo chromatin expansion, nuclear membrane rupture, and eventual cell membrane breakdown.

The successful categorization and clustering of activation stages were validated through the analysis of clinical samples from both healthy controls and fever patients. The model demonstrated a significant increase in activated leukocytes among fever patients, with an average of 32.38% activation compared to 5.41% in healthy controls. This disparity underscores the model's ability to discern subtle variations in immune response, crucial for early diagnosis and treatment monitoring of inflammatory conditions. Although the differential blood count values were within the normal range, our system detected a significant increase in activated leukocytes. This implies that modern haematology analysers are insufficient of differentiating this potentially clinically useful parameter.

Importantly, the study highlighted the variability in immune responses among fever patients. This variability suggests that individual patients' cellular response is a possible target for a more personalised treatment based on the relative activation score of the innate immune system. For instance, the potential clinical outcome of developing a leukocyte activation assay could have significant implications for understanding monocyte activation in viral infections such as COVID-19 [12]. Point of care assessment of activation level of the innate immune system makes it possible to monitor disease severity early and

the risk of potentially lethal complications which currently suffers from the inability of clinicians to separate patients with immunosuppression or a hype hyperreagible immune system.

Our findings validate the potential of DHM combined with deep learning as a powerful tool for real-time, label-free monitoring of leukocyte activation. This technology could enable timely interventions and more accurate monitoring of disease progression and treatment efficacy. However, further validation with larger cohorts is necessary to fully realize this approach's potential. Expanding the sample size will enhance the robustness of our model and its applicability across diverse patient populations. Future studies should aim to include a broader array of clinical conditions to establish the generalizability of our findings. Additionally, exploring the composition of the training set comprised of different leukocyte subtypes on model performance will provide deeper insights into the nuances of immune response monitoring.

In conclusion, integrating DHM with deep learning algorithms represents a promising advancement in cellular imaging and immune response analysis. This approach can revolutionize diagnostic and therapeutic strategies for a wide range of inflammatory and immune-related conditions by providing detailed, real-time insights into leukocyte activation. Moreover, the unmet need for an activation assay to evaluate patient risk in acute care settings, particularly in conditions like COVID-19, highlights the significance of our findings in identifying early predictive biomarkers for immune cell activation.

## Acknowledgements

This work was supported by the Singapore National Research Foundation through its thematic Campus for Research Excellence and Technological Enterprise (CREATE) grant RF2019-THE002-0008.

## References

- [1] R. F. Kraus and M. A. Gruber, "Neutrophils-From Bone Marrow to First-Line Defense of the Innate Immune System," *Front Immunol*, vol. 12, p. 767175, 2021, doi: 10.3389/fimmu.2021.767175.
- [2] J. Austermann, J. Roth, and K. Barczyk-Kahlert, "The Good and the Bad: Monocytes' and Macrophages' Diverse Functions in Inflammation," *Cells*, vol. 11, no. 12, Jun 20 2022, doi: 10.3390/cells11121979.
- [3] P. Kruger, M. Saffarzadeh, A. N. R. Weber, N. Rieber, M. Radsak, H. V. Bernuth, C. Benarafa, D. Roos, J. Skokowa, and D. Hartl, "Neutrophils: Between host defence, immune modulation, and tissue injury" (in eng), *PLoS Pathog*, vol. 11, no. 3, p. e1004651, Mar 2015, doi: 10.1371/journal.ppat.1004651.
- [4] M. Gutierrez-Arcelus, S. S. Rich, and S. Raychaudhuri, "Autoimmune diseases - connecting risk alleles with molecular traits of the immune system," (in eng), *Nat Rev Genet*, vol. 17, no. 3, pp. 160-74, Mar 2016, doi: 10.1038/nrg.2015.33.
- [5] S. Mol, F. M. J. Hafkamp, L. Varela, N. Simkhada, E. W. T. Kueter, S. W. Tas, M. H. M. Wauben, T. G. Kormelink and E. C. Jong, "Efficient Neutrophil Activation Requires Two Simultaneous Activating Stimuli" *Int J Mol Sci*, vol. 22, no. 18, Sep 18 2021, doi: 10.3390/ijms221810106.
- [6] I. Kwiecień, E. Rutkowska, K. Gawroński, K. Kulik, A. Dudzik, A. Zakrzewska, A. Raniszewska, W. Sawicki, and P. Rzepecki, "Usefulness of New Neutrophil-Related Hematologic Parameters in Patients with Myelodysplastic Syndrome" *Cancers (Basel)*, vol. 15, no. 9, Apr 26 2023, doi: 10.3390/cancers15092488.
- [7] M. Kono, K. Saigo, S. Matsuhira, T. Takahashi, M. Hashimoto, A. Obuchi, S. Imoto, T. Nishiyama, S. Kawano, "Detection of activated neutrophils by reactive oxygen species production using a hematology analyzer" *J Immunol Methods*, vol. 463, pp. 122-126, Dec 2018, doi: 10.1016/j.jim.2018.10.004.
- [8] M. Ugele, M. Weniger, M. Stanzel, M. Bassler, S. W. Krause, O. Friedrich, O. Hayden, L. Richter, "Label-Free High-Throughput Leukemia Detection by Holographic Microscopy" *Advanced Science*, vol. 5, no. 12, p. 1800761, 2018, doi: <https://doi.org/10.1002/advs.201800761>.
- [9] C. Y. F. Dubois, "Off-axis interferometer," 06.07.2016.
- [10] *Ultralytics YOLOv8*. (2023). [Online]. Available: <https://github.com/ultralytics/ultralytics>
- [11] E. Neubert, D. Meyer, F. Rocca, G. Günay, A. K. Tessmann, J. Grandke, S. S. Sander, C. Geisler, A. Egner, M. P. Schön, L. Erpenbeck and S. Kruss, "Chromatin swelling drives neutrophil extracellular trap release" *Nat Commun*, vol. 9, no. 1, p. 3767, Sep 14 2018, doi: 10.1038/s41467-018-06263-5.
- [12] E. A. Ivanova and A. N. Orekhov, "Monocyte Activation in Immunopathology: Cellular Test for Development of Diagnostics and Therapy," *J Immunol Res*, vol. 2016, p. 4789279, 2016, doi: 10.1155/2016/4789279.